# Nonlinear magneto-optical rotation – A possible tool for sensitive magnetometry

*R. Srinivasan*

*Optical pumping in an alkali metal vapour produces long-standing coherences of ground state Zeeman sub-levels. These coherences produce large nonlinear magneto-optic rotation (NMOR). Techniques using optical coherences for sensitive magnetometry have been in vogue for a long time. However, the sensitivity achieved has been three orders of magnitude lower than that of a SQUID magnetometer. The NMOR technique has yielded signals having a very narrow width of a few micro-Gauss. In principle, it has been demonstrated that with NMOR magnetometers one can obtain a sensitivity matching, or better than the sensitivity of a Squid magnetometer. There are still many problems to be resolved before these magnetometers can be put to use in geomagnetic and biological applications, where small magnetic fields need to be measured.*

**Keywords:** Magnetometry, nonlinear magneto-optic rotation, optical coherence.

WHEN an atom or a nucleus having a magnetic moment is placed in a magnetic field, the magnetic moment precesses about the field at the Larmor precession frequency. A measurement of the Larmor precession frequency of an atom or nucleus with a known magnetic moment enables one to deduce the value of the magnetic field. In nuclear magnetic resonance (NMR), one applies a weak radiofrequency signal to the sample in a magnetic field. When the frequency of this signal matches the Larmor precession frequency of the nuclear magnetic moment, maximum energy of the signal is absorbed.

NMR is used extensively in magnetic resonance imaging. The equipment is bulky and costly. One can produce a magnetic alignment of atomic spins by optical techniques instead of using a magnetic field produced by a bulky coil. One can also detect the Larmor precession frequency in a weak magnetic field using optical techniques. Optical magnetometry has been a subject of study for several decades. Lack of space prevents us from discussing these studies even briefly. An example of an application of an all-optical magnetometer is its use for electrocardiography[1]. These magnetometers have achieved a maximum sensitivity of the order of $10^{-8}$ G/$\sqrt{\text{Hz}}$. The sensitivity of a Squid magnetometer is three orders of magnitude higher. With nonlinear magneto-optic rotation (NMOR), one can achieve a Shot noise limited sensitivity rivalling that of a Squid magnetometer.

This article is a brief review of the recent developments in NMOR. Limitations of space prevent a discussion of various nonlinear magneto-optical effects such as the Hanle effect, level-crossing spectroscopy, etc. The interested reader may like to consult the detailed review articles by Budker *et al.*[2] and Alexandrov *et al.*[3]. To make this article intelligible and self-contained, a few basic concepts need to be presented. This is done in the next section.

R. Srinivasan is in the Raman Research Institute, C. V. Raman Avenue, Sadashivanagar, Bangalore 560 080, India.
e-mail: rsv@rri.res.in

## Basic concepts necessary to understand NMOR

Let us consider an ensemble of atoms. Let the atom have a ground state with the total angular momentum quantum number F = 1 and an excited state F′ = 1. A state with a total angular momentum F has (2F + 1) degenerate sub-levels, with the projection of the angular momentum along the axis of quantization described by a quantum number $m_F$ going from –F to +F in steps of unity. The energy separation between the ground and excited levels is $\hbar\omega_0$, where $\hbar$ is the Planck constant divided by $2\pi$ and $\omega_0$ is the circular frequency of the transition. Usually $\omega_0$ is in the optical region. Even at room temperature, the ratio $\hbar\omega_0/k_BT$ is so large that almost all the atoms populate only the ground state sub-levels with equal probability. A negligible fraction of the atoms is to be found in the excited state.

The energy level diagram of the atom is shown in Figure 1. When a light beam of frequency $\omega$ (detuning $\delta$ of the light beam is $\omega - \omega_0$) is incident on a gas of atoms, there will be a velocity class of atoms for which the Doppler shift exactly cancels the detuning. The light beam will be in exact resonance. This will cause a depletion of the atoms in the ground state with this velocity class because the light beam raises these atoms to the excited levels at a rapid rate. Such selective excitation will cause narrow spectral features in absorption as well as in magneto-optic rotation with a width of a few MHz, corresponding to the lifetime of the atoms in the excited state. These are called Bennet structure

effects. When the magnetic field is varied, these Bennet structures in MOR will show a width of the order of a Gauss. We will not be dealing with these effects. We will deal only with coherence effects in the ground state. How these are produced is explained below.

Let left circularly ($\sigma^+$) polarized light, travelling along the axis of quantization (which we call as the *y*-axis), fall on this ensemble of atoms. The selection rule for absorption of this light is $F' - F = \pm 1$, or 0 and $m_{F'} - m_F = +1$. So this light will raise the atoms in the ground sub-levels $m_F = 0$ and $m_F = -1$ to the excited sublevels $m_{F'} = +1$ and $m_{F'} = 0$ respectively. The atoms in the ground state sub-level $m_F = +1$ will not absorb this light. The atoms raised to the excited states remain in those states for a short time (of the order of a few nano-seconds) and then come down to the ground sub-levels by spontaneous emission. The selection rule for this process is $m_F' - m_F = +1$, 0 or –1. So atoms from $m_{F'} = 1$ can come down to $m_F = 0$ or $m_F = +1$, while those in the excited sub-level $m_F = 0$ can come down to all the three ground state sub-levels. The number of absorption-spontaneous emission cycles per second will depend on the detuning and the intensity of the light. If the detuning is a few mega Hertz and the intensity of the incident light is not too low (i.e. the intensity is several hundred $\mu W/cm^2$), the number of such transitions will be of the order of $10^4$ to $10^6$ per second. From the above discussion it is obvious that during these many absorption-spontaneous emission cycles, the populations in the ground state sub-levels $m_F = 0$ and –1 are progressively depleted and the population in the ground state sub-level $m_F = +1$ grows. In a time of the order of a few hundreds of micro-seconds to a few milliseconds, all the atoms in the ground state will be transferred to the sub-level $m_F = +1$. This re-distribution of atoms among the ground state sub-levels due to the incident light is called optical pumping.

The atoms in the ground state $m_F = +1$ have the maximum projection $m_F = F$ along the axis of quantization. The atoms in the ensemble in the state $m_F = +1$ are said to be in an oriented state. The ensemble in the oriented state will also have a non-zero magnetic moment along the axis of quantization. The ensemble exhibits a magnetic dipole moment purely arising out of optical pumping, even in the absence of an applied magnetic field.

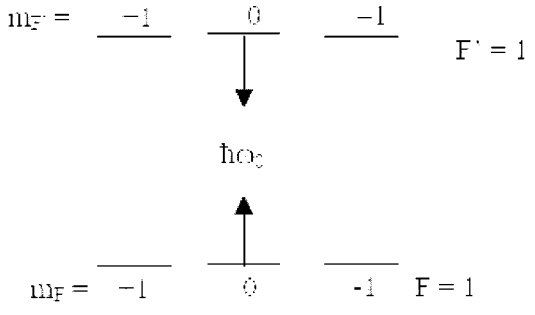


**Figure 1.** Energy level diagram of an atom with F = 1 and F′ = 1.

If the incident light is right circularly ($\sigma^-$) polarized, the selection rule for absorption is $m_{F'} - m_F = -1$. An argument analogous to the one in the above paragraph leads to the conclusion that optical pumping will transfer all the atoms to the ground state sub-level $m_F = -1$. The atoms in state $m_F = -1$ are again in an oriented state, which is different from the one produced by $\sigma^+$ polarized light. The oriented state produced thus will be destroyed only by collisions of the atoms with themselves, or with atoms of another species present, or by collisions with the walls of the vessel. At low pressures, at which the mean free-path of the atom is large compared to the dimensions of the containing vessel, the collision with the wall is the most important mechanism determining the lifetime of the oriented state.

Let us say we have produced the oriented state with the atoms in the $m_F = +1$ ground state. If we now shine a weak $\sigma^+$ light beam on this ensemble of atoms, it will not be absorbed because such absorption will violate the selection rule for this polarization. On the other hand, if the weak light beam is $\sigma^-$ polarized, the light will be absorbed because such absorption will not violate the selection rule for $\sigma^-$ polarization. Thus the absorption coefficients for the two different circularly polarized states will be different. This phenomenon is known as circular dichroism. Accompanying this phenomenon, the real part of the refractive index also will be different for the two circular states of polarization. This is called circular birefringence. If linearly polarized light is sent through such an oriented ensemble, circular birefringence will cause a rotation of the plane of polarization. This effect is similar to the rotation of plane of polarization of a light beam when a magnetic field is applied to a medium through which the light passes. This phenomenon is known as Faraday rotation.

Let us consider a second situation. Here the light beam is travelling along the *Z*-axis perpendicular to the axis of quantization. The beam is linearly polarized. The electric vector of the light beam may be perpendicular to the axis of quantization (i.e. along the *X*-axis) or parallel to the axis of quantization (i.e. *Y*-axis). In the former case, the light beam is said to be $\sigma$-polarized and in the latter it is said to be $\pi$-polarized. For $\sigma$-polarized light the selection rule for absorption is $m_{F'} - m_F = \pm 1$. This is because we may consider the $\sigma$-polarized light to be a superposition of two circular components, one being $\sigma^+$ polarized and the other $\sigma^-$ polarized. An atom in the ground sub-level $m_F = +1$ will be excited to the sub-level $m_{F'} = 0$ by the $\sigma^-$ component. The $\sigma^+$-component causes an induced emission from $m_{F'} = 0$ to $m_F = -1$. This second-order process couples the two levels. Instead of the two degenerate sub-levels $m_F = +1$ and –1, we may choose two other degenerate sublevels

$$|+> = (1/\sqrt{2})(|m_F = 1> + |m_F = -1>), \quad (1)$$

$$|-> = (1/\sqrt{2})\,(|m_F = 1> - |m_F = -1>). \quad (2)$$

The two states are coherent superpositions of the two ground states $m_F = +1$ and $m_F = -1$.

One can see that the transition matrix element connecting the state $|->$ to $m_{F'} = 0$ vanishes because of the minus sign within the brackets in eq. (2). The transition amplitudes from $m_F = 1$ and $m_F = -1$ to $m_{F'} = 0$ interfere destructively. When atoms are pumped by optical pumping to the state $|->$ the incident $\sigma$-polarized light can no longer raise the atoms from $|->$ to $m_{F'} = 0$ state. Due to the incident light, atoms in all the ground sub-levels $m_F = 1$, 0 and $-1$ are raised to the excited levels and then fall back to the levels $+>$, $|->$ and $m_F = 0$ as coherence develops. The atoms in the level $|->$ are no more affected by the incident light while atoms in the other two ground levels will be affected. In the course of time all atoms will be optically pumped to the state $|->$. An ensemble of atoms produced thus will have no net projection of angular momentum along the axis of quantization. This is not an oriented state. This state is called an aligned state for the following reason.

Suppose we have created the aligned state in which the atoms are in the ground state sublevel $|->$. We have already seen that an incident weak $\sigma$-polarized beam will not be absorbed by the atoms in this state. But a weak $\pi$-polarized beam, for which the selection rule for the transition is $m_{F'} = m_F$, will be absorbed as the transition probability from $|->$ to the excited sub-levels is nonzero for this state of polarization. Thus the two light beams polarized in mutually perpendicular directions will have different absorptions. This is called linear dichroism. Since the properties of the ensemble are different in different directions, this state is called an aligned state.

The properties of the ensemble of atoms in the ground sub-levels are described by the $(2F + 1) \times (2F + 1)$ density matrix $\rho$. The diagonal elements $<m_F|\rho|m_F>$ indicate the fraction of atoms in the sub-level $m_F$, while the non-diagonal matrix element $<m'_F|\rho|m_F>$ is a measure of the coherence between the states $m'_F$ and $m_F$. If the ensemble is in an incoherent mixture of states (e.g. an ensemble in thermal equilibrium), the non-diagonal elements of the density matrix are zero. When coherence is established by the $\sigma$-polarized light as in the example cited above, the non-diagonal element $<1|\rho|-1>$ is nonzero.

In the presence of a magnetic field or an electric field that interacts with the atoms through an interaction Hamiltonian $H_I$, the density matrix evolves with time according to the equation

$$d\rho/dt = (i/\hbar)\,[H, \rho]. \qquad (3)$$

Here $H$ is the Hamiltonian, including the interaction and the square brackets indicate the commutator.

In a magnetic field, this evolution is simple. The angular momentum vector **F** precesses about the direction of the magnetic field **B** with the Larmor precession frequency $\Omega_L = eB/m$, where $e$ and $m$ are the charge and mass of the electron.

It will be good to visualize the effect of the precession on the oriented or aligned state. A convenient method of visualizing these states is described by Rochester and Budker[4]. In this method one plots along a direction $(\theta, \phi)$, a line of length $r$ proportional to the probability of finding the projection $m_F$ to be equal to $F$ along that direction. The tips of such lines define a surface that figuratively represents the oriented or aligned state. For example, Figure 2 *a* represents an oriented state along the direction *y*. In Figure 2 *a* we see that the probability of finding $m_F = F$ is maximum in the *y*-direction and becomes zero for a direction making an angle of 90° or more with the *y*-axis. Figure 2 *b* visualizes an aligned state corresponding to a transition from F = 1 to F′ = 1. We see that along the *x*-direction the probability of finding a projection $m_F$ = F is nil while along *y*- and *z*-directions the probability is maximum. Note that Figure 2 *a* representing an oriented state does not have inversion symmetry about the origin, while Figure 2 *b* representing the aligned state has this symmetry.

Once we have visualized an oriented or an aligned state, it will be easy to see what happens to the figure due to the time evolution of the density matrix. The power of this

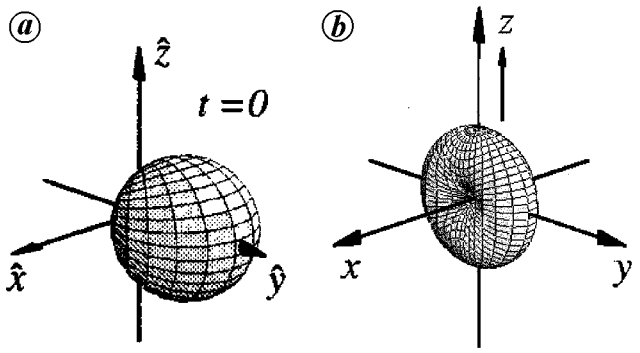


**Figure 2.** Visualization of (***a***) an oriented state and (***b***) an aligned state of an atom.

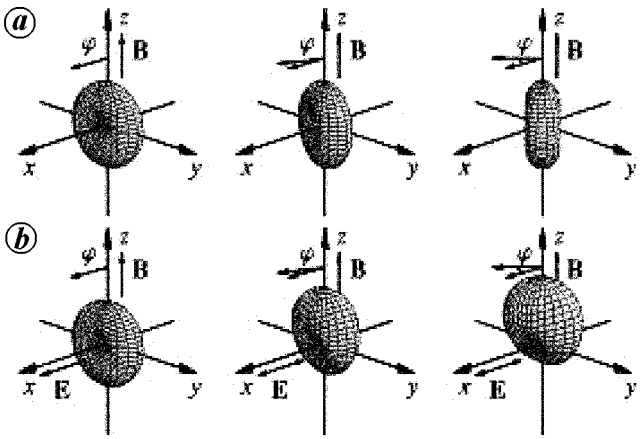


**Figure 3.** Sequences showing the evolution of optically pumped ground-state atomic alignment in a longitudinal magnetic field for an F = 1–F′ = 1 transition at low and high light powers (time proceeds from left to right). The distance from the surface to the origin represents the probability of finding the projection $M$ = F along the radial direction. Reprinted figure with permission from D. Budker *et al*.. *Rev. Mod. Phys*., Vol. 74, 1153 (2002). Copyright (2002) by the American Physical Society.

method is illustrated in Figure 3. This figure illustrates how the aligned state described in the text above develops as a function of time in an applied magnetic field. If the light intensity is weak, so that only the interaction of the atom with the magnetic field is included in the Hamiltonian, the aligned state precesses about the magnetic field $B$ along the $Z$-axis as shown in the sequence of Figure in 3 *a*. The magnetic field causes the Zeeman sub-levels $m_F = \pm 1$ to be shifted by $\pm \hbar\Omega_L$. The time evolution of the levels at these frequencies is responsible for Larmor precession.

However, if the intensity of the light beam is high, then we should also involve the interaction of the atoms with the electric field of the light beam. This will produce an AC Stark shift of the atomic sub-levels. These shifts in energy will cause the different sub-levels in the superposed state |–> to have time evolutions different from those caused by the magnetic field. This leads to a change in the time evolution of the aligned state from a simple precession about the magnetic field. This sequence is shown in Figure 3 *b*. Note that Figure 3 *b* differs from Figure 3 *a* in one important respect. In Figure 3 *a*, the figure representing the state of the ensemble retains the inversion symmetry at all time. In Figure 3 *b*, this is not true. We see here that the state changes partially from an aligned to an oriented state. This implies that the aligned state which did not have a net magnetic moment at $t = 0$ changes with time to a state which develops a nonzero magnetic moment. This is called alignment to orientation conversion.

We have now introduced all the ideas necessary for a discussion of NMOR. But before we go on to a discussion of NMOR, a few words will be in order about linear MOR.

## Linear MOR – Faraday rotation

The rotation of the plane of polarization of linearly polarized light passing through a medium along a longitudinal magnetic field is known as the Faraday effect, which was discovered nearly 150 years ago. The magnetic field produces an oriented state in which we have circular birefringence. A weak linearly polarized light beam passes along the direction of the magnetic field. The linear polarization can be decomposed into two circular polarizations, $\sigma^+$ and $\sigma^-$ of equal amplitude. Due to the circular birefringence these two waves travel with different phase velocities in the medium. When they emerge after travelling a length $L$ in the medium, they will have a phase difference

$$\phi = 2\pi(\Delta n L/\lambda). \quad (4)$$

$\Delta n$ is the difference in refractive indices of the two circularly polarized components and $\lambda$ is the wavelength of light. The superposition of these two circular components with a phase difference $\phi$ leads to a linear polarized light beam with its plane of polarization rotated relative to that of the incident beam by

$$\varphi = \phi/2. \quad (5)$$

This is the explanation of Faraday rotation. The birefringence is proportional to the applied magnetic field $B$. The ratio $\varphi/BL$ is a constant for the medium, called the Verdet constant. The Verdet constant will vary with the wavelength of the incident light. The magnitude of the Verdet constant is about $10^{-5}$ radians/Gauss/cm in dense flint glasses.

When the incident light is resonant to an atomic transition, the magneto-optical rotation in a longitudinal magnetic field is called the Macaluso–Corbino effect[5]. On resonance the dispersion of the rotation angle $\varphi$ with the longitudinal magnetic field B is given by

$$\varphi = 2(g\mu B/\Gamma)[|(1 + \imath 2(\delta/\Gamma))|^2 + (2g\mu B/\Gamma)^2]. \quad (6)$$

Here $g$ is the Landé factor, $\mu$ the magnetic moment and $\Gamma$ the relaxation rate of the excited state and $\imath = \sqrt{(-1)}$.

One sees from eq. (6) that when the light is far detuned the effect of $B$ in the denominator is negligible and the rotation $\varphi$ is proportional to $B$. As the detuning $\delta$ decreases the magneto-optic rotation increases and is a maximum at resonance $\delta = 0$. At resonance the variation of $\varphi$ with B shows a dispersion-like behaviour. It has a negative value for a negative value of $B$. As $B$ is made more positive, the rotation shows a negative maximum value when

$$|2g\mu B| = \Gamma. \quad (7)$$

As $B$ is made more positive, the magnitude of $\varphi$ decreases and passes through zero when $B$ is zero. A further increase in $B$ results in a positive rotation angle $\varphi$ that increases with $B$, passes through a maximum when eq. (7) is satisfied and decreases to zero as $B$ is increased to very high values.

NMOR per atom is several orders of magnitude larger than linear Faraday rotation and can provide very high sensitivity for magnetic field measurements. In linear MOR, the probe light beam interacts only to the first order in perturbation with a medium that is produced in an oriented state by a magnetic field. In NMOR, the perturbation of light with the medium is taken to orders higher than the first. The oriented or aligned state itself is produced by a pump light beam and the probe beam is then influenced by the modified optical properties of the oriented or aligned medium.

## Mechanism for NMOR

NMOR can be understood on the basis of the 'rotating polarizer' model. In this model three stages are invoked

in producing MOR. In the first stage the pump beam, which is linearly polarized, produces an aligned state in a thin layer of atoms. The aligned state exhibits linear dichroism for light travelling along the *Z*-axis. If a magnetic field *B* is applied along *Z*, this aligned state precesses with the Larmor precession frequency $\Omega_L$. This precession is shown in Figure 3 *a* and causes the principal axes of dichroism to rotate about the *Z*-axis. When the layer of atoms in this aligned state enters the probe beam, linearly polarized in the same direction as the pump light, the electric vector of the probe beam is resolved into two components $E_{\|}$ and $E_{\perp}$ along the principal dichroic axes of the atomic layer (Figure 4). These principal axes are rotated from their original direction by an angle $\theta = \Omega_L \tau$, where $\tau$ is the time taken by the atoms to travel from the pump to the probe region. The thin layer acts as a rotating, linearly dichroic polarizer. Hence the name rotating polarizer model. Because the absorption for the two components of the electric field vector differs, the ratio of the two components gets altered when the light passes through the layer of aligned atoms. The two components now combine together to give linearly polarized light. The direction of linear polarization is rotated relative to the direction of polarization of the incident light. This is the mechanism of NMOR shown in Figure 4.

It is not necessary to have separate pump and probe beams. The pump beam can also serve as the probe beam. The intensity of the pump beam need not be very high to produce NMOR. Whether nonlinear magneto-optical effects will be produced or not depends on the value of the saturation parameter defined as

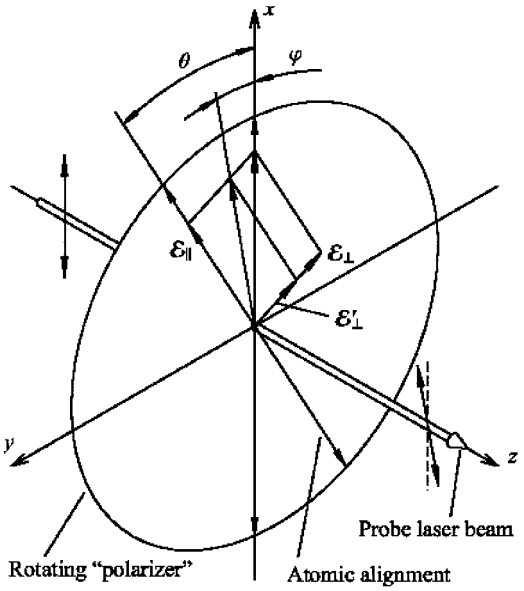


**Figure 4.** An optically thin sample of aligned atoms precessing in a magnetic field, which can be thought of as a thin, rotating polaroid film that is transparent to light polarized along its axis ($E_{\|}$) and slightly absorbent for the orthogonal polarization ($E_{\perp}$). Reprinted figure with permission from D. Budker *et al*.. *Rev. Mod. Phys*., Vol. 74, 1153 (2002). Copyright (2002) by the American Physical Society.

$$\kappa = \Omega_R^2/\Gamma\gamma. \quad (8)$$

Here $\Omega_R$ is the Rabi frequency of the pump light ($\Omega_R = |d \cdot E|/\hbar$, where *d* is the dipole moment for the transition and *E* is the amplitude of the electric field of the incident light beam) and $\Gamma$ is the reciprocal of the lifetime of the excited state. $\Omega_R^2/\Gamma$ is the rate of optical pumping and $\gamma$ is the relaxation rate of the ground-state coherence. Ground-state coherence is long-lived (of the order of a few tens of milliseconds or more) and so $\gamma$ is small. Since $\gamma$ is small, one can observe nonlinear effects even at low intensities.

Calculations performed by Kanorsky *et al*.[6] based on the rotating polarizer model have been successful in giving a quantitative fit to the line shapes at low intensities of the pump beam, both for longitudinal and transverse magnetic fields. At resonance ($\delta = 0$) (resonance can be followed by a simultaneous recording of the fluorescence intensity from the transition), the variation of $\varphi$ with *B* follows eq. (6) with $\delta = 0$ and $\Gamma$ replaced by $\gamma$. Hence one can get very narrow line widths by reducing $\gamma$.

As the intensity of the light beam is increased, an alignment to orientation conversion takes place with time as shown in Figure 3 *b*. The orientation component enhances the NMOR. In sensitive magnetometers, light intensities have a magnitude large enough to cause such a conversion.

## Relaxation rate of ground-state coherence and NMOR line width

When we talk about narrow resonances here we should be clear about what we mean. We are not changing the frequency of the incident light beam. It is at a fixed detuning from the transition frequency. We are changing the magnetic field and the signal shows a dispersion-like behaviour with narrow peaks both on the negative and positive sides of the zero of magnetic field. These peaks occur at a magnetic field *B* for which the Larmor precession frequency matches the inverse lifetime for the relaxation of the ground-state coherence.

The width of the NMOR resonance signal depends on the value of $\gamma$, i.e. the transverse spin relaxation rate. There are several contributions to this rate, such as (a) spin exchange collision rate between the alkali atoms, (b) spin destroying collision rate between the alkali atoms themselves, and the alkali atoms and the buffer gas atoms in the vapour cell and (c) collisions with the walls which may contain paramagnetic or ferromagnetic impurities. To get a narrow line width, $\gamma$ should be made small.

In a vapour cell containing only the alkali atoms at a density of about $10^9$/cc, the mean free path is larger than the dimension of the cell. So polarization destruction arises only through collision of the atom with the wall of the cell. In such a case atoms will enter the pump beam in the unpolarized state every time. The line width will be deter-

mined by the time the atom takes to go from the pump to the probe region. When a single beam is used as a pump and probe, the relevant relaxation time is the transit time for the atom to cross the width of the beam. This will give rise to a width of the resonance line of the order of a hundred milli-Gauss at low intensities of light.

One may use an atomic beam, and separate the pump and probe beams. With such an arrangement, polarization relaxation time $\tau$ will depend on the separation between the beams, and the velocity of the atoms. Such spectrometry with separated pump and probe beams is called Faraday–Ramsey spectrometry. Using a Cs atom beam, narrow signals with a width of 1 milli-Gauss have been obtained with a separation of 30 cm between the pump and probe beams[7].

One may also increase the relaxation time by laser cooling the atoms and using a fountain of cold atoms for the experiment[8,9].

An effective technique to reduce $\gamma$ is to coat the walls of the vapour cell with antirelaxation coating of paraffin[10,11]. With such a coating, the polarization of the atom is preserved when it collides with the wall. Such paraffin-coated walls have been shown to be stable for as long as 40 years[12]. An atom, after leaving the pump beam, will suffer several thousand velocity-changing collisions with the wall without relaxing its polarization state and can then return to the probing region. This will increase the time between pumping and probing enormously, thereby increasing the NMOR and decreasing the width of the resonance line[13]. This is called wall-induced Ramsey effect. Resonance line as narrow as a few micro-Gauss has been observed with $^{85}$Rb in an antireflection-coated cell by Budker *et al.*[14]. This is shown in Figure 5. In this experiment the incident light intensity

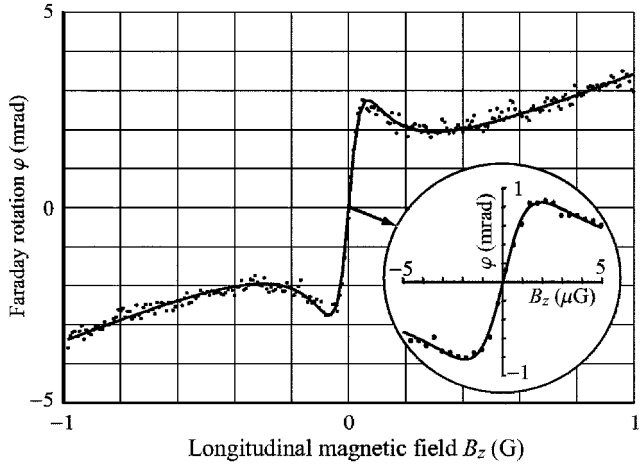


**Figure 5.** Longitudinal magnetic-field dependence of optical rotation in a paraffin-coated $^{85}$Rb-vapour cell. The background slope is due to the Bennett-structure effect. The dispersion-like structure is due to the transit effect. (Inset) Near zero $B_z$-field behaviour at a $2 \times 10^5$ magnification of the magnetic-field scale. Light of intensity 100 μW/cm$^2$ is tuned 150 MHz to the high frequency side of the F = 3 $\tau$o F′ absorption peak. Reprinted figure with permission from D. Budker *et al*.. *Rev. Mod. Phys*., Vol. 74, 1153 (2002). Copyright (2002) by the American Physical Society.

was 100 μW/cm$^2$. When the light intensity is increased, the signal saturates at some value of the intensity due to power broadening.

An important parameter is the sensitivity of a magnetometer, defined as the smallest value, $\delta B$, of the magnetic field it can detect. If NMOR is used for detection of the magnetic field, then

$$\delta B = (\partial\varphi/\partial B)^{-1}\delta\varphi. \quad (9)$$

A high sensitivity will be obtained if the peak signal value is large and the width of the signal is small making $\partial\varphi/\partial B$ large. $\delta\varphi$ is the smallest rotation angle that can be measured. For Shot noise limited detection with a measurement time $t_m$

$$\delta\varphi = (1/2)\sqrt{h\nu/Pt_m}. \quad (10)$$

$\nu$ is the frequency of the laser light and $P$ is the power transmitted through the cell.

Budker *et al.*[15] optimized the slope ($\partial\varphi/\partial B$) for zero magnetic field in $^{85}$Rb vapour in a cell coated with paraffin by varying the detuning and the intensity of the beam and found the best Shot noise limited sensitivity of $3 \times 10^{-12}$ Gauss/√Hz. The sensitivity of a Squid magnetometer is around $10^{-11}$/Gauss/√Hz. The sensitivity of the NMOR magnetometer compares favourably with the sensitivity of a Squid magnetometer.

One may use a higher density of alkali atoms and increase the intensity of the incident beam to produce large Zeeman coherences. This will enhance the NMOR signal. However, one will have to use a buffer gas in the cell to reduce the spin-exchange collision rates between the alkali atoms. Using an alkali vapour density of $10^{12}$ atoms and a buffer gas of Ne at a pressure of 3 Torr, Sautenkov *et al.*[16] showed that the NMOR signal was enhanced by several orders of magnitude. However, the sensitivity was reduced.

## Synchronous optical pumping polarimetry

To see narrow features from a few micro-Gauss to a few hundred milli-Gauss (necessary for varied applications such as bio-magnetic and geo-magnetic measurements), it will be convenient to use synchronous optical pumping[17]. In this technique the laser frequency or amplitude is modulated at a frequency $\Omega_m$. One can modulate the frequency of the laser light at a few kilo Hertz by giving a suitable AC signal to the piezo that will turn the grating to and fro in an external cavity diode laser. To modulate at a much higher frequency, the current through the diode can be varied at this frequency. The amplitude of frequency modulation must be several hundred mega Hertz, of the order of the Doppler width. Amplitude modulation of the pumping beam can be achieved using an acousto-optic modulator/deflector that will deflect the beam periodically at the desired frequency. The aligned state, precess-

ing in the applied magnetic field at the Larmor precession frequency $\Omega_L$, causes the linear dichroic properties of the ensemble to oscillate at frequency $2\Omega_L$. The factor 2 arises because of the inversion symmetry of the polar diagram. Modulation of either the detuning or the intensity of the light beam causes the polarization of the ensemble to change at the frequency $\Omega_m$. If the modulated optical rotatory signal is detected with a lock-in amplifier, one gets a sharp resonance both in the in-phase and quadrature signals when $\Omega_m = 2\Omega_L$. If one looks in the second harmonic channel of the lock-in, then a resonance signal is seen when $\Omega_m = \Omega_L$. A measurement of $\Omega_m$ at which a resonance is seen gives the value of the magnetic field. Since the Larmor precession frequency is measured, this technique of measuring the magnetic field is absolute and does not need calibration.

A typical experimental set-up using synchronous optical pumping with frequency-modulated light described by Budker *et al.*[18] is shown in Figure 6.

A paraffin-coated cell of diameter 10 cm filled with enriched $^{87}$Rb at a density of a few $10^9$ atoms/cc is kept within four layers of magnetic shielding of a ferromagnetic metal. This provides a shielding by a factor of $10^6$ to external fields. A spherical shape of the shield will effectively shield all the components of stray magnetic fields. But such a shape is difficult to fabricate. The details of construction of the shield are described in Yashchuk et *al.*[19]. The cell is surrounded by seven coils within the shield, which compensate for any stray residual magnetic field components $B_x$, $B_y$, $B_z$, the first derivatives $dB_x/dx$, $dB_y/dy$, $dB_z/dz$ and the second derivative $d^2B_z/dz^2$. Light from an external cavity diode laser is frequency-modulated. It then passes through a polarizer and the cell, and is incident on a polarizing beam splitter analyser set with its axis at 45° to the incident light beam. The split beams fall on photodiodes PD1 and PD2 and the signals are measured in the first or second harmonic of the modulation frequency by the lock-in amplifier. After the average stray field over the volume of the cell is nullified to within 0.1 μGauss, one can apply any longitudinal field by changing the current through the respective coil.

Figure 7 shows the signals obtained for a modulating frequency of 1 kHz, as the longitudinal magnetic field was varied. Signals are shown both in the first and second harmonic channels.

For measuring magnetic fields of the order of a few hundred milli-Gauss to about 1 Gauss, one should modulate the light beam at a frequency of the order of $10^5$ to $10^6$ Hz. This is the field range for geomagnetic applications. Acosta *et al.*[20] have studied the resonance signals from $^{87}$Rb in this range of fields. This atom in the ground state F = 2 shows the first harmonic signal for a longitudinal field of 405 milli-Gauss. One clearly sees the splitting of the signal into three components. This splitting will increase the width of the overall resonance curve and thereby reduce the sensitivity of measurement of fields around resonance. The authors estimated a Shot noise limited sensitivity of $6 \times 10^{-10}$ G/√Hz.

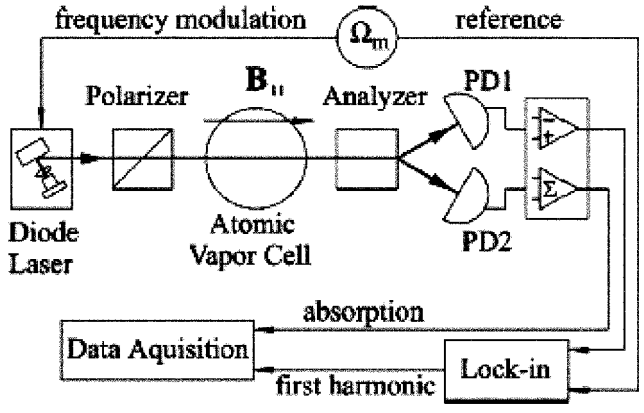


**Figure 6.** Simplified schematic of the apparatus. Reprinted figure with permission from D. Budker *et al.*. *Phys. Rev. A*, Vol. 65, 055403 (2003). Copyright (2003) by the American Physical Society.

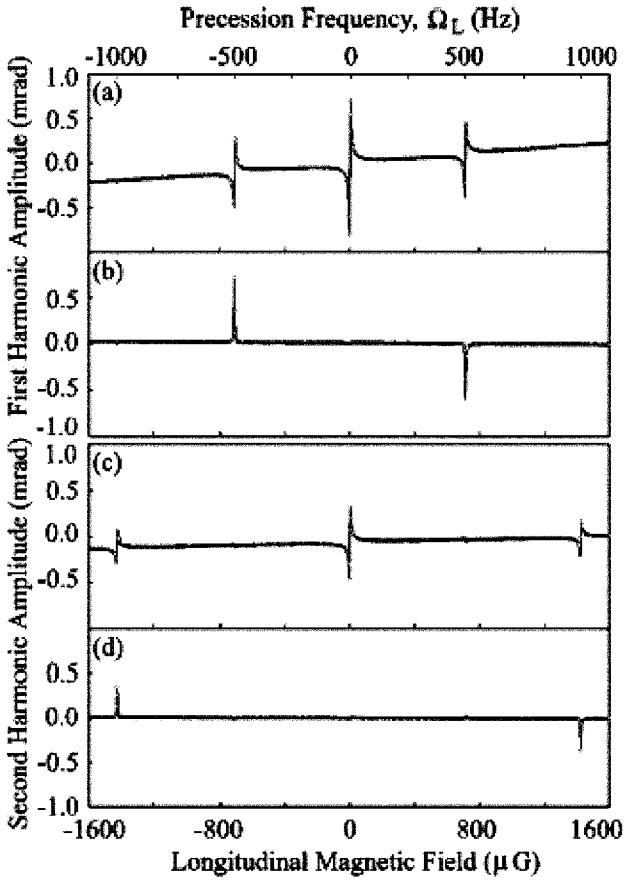


**Figure 7.** Signals detected at the first harmonic (a), (b) and second harmonic (c), (d) of $\Omega_m$ as a function of longitudinal magnetic field. The laser power was 15 μW, beam diameter 2 mm, $\Omega_m = 2\pi \times 1$ kHz, and $\Delta\omega = 2\pi \times 220$ MHz. Traces (a), (c) and (b), (d) correspond to the in-phase and the quadrature outputs of the signals from the lock-in detector respectively. Reprinted figure with permission from D. Budker *et al.*. *Phys. Rev. A*, Vol. 65, 055403 (2003). Copyright (2003) by the American Physical Society.

The experiments described above use the aligned state of polarization, cells of large volume, alkali atoms at a low density and light beams of low power. A magnetometer based on the precession of alignment is a scalar magnetometer. It will measure the total value of the magnetic field, but not the individual components.

## High sensitivity magnetometer unaffected by spin exchange relaxation

Allred *et al.*[21] have described a high-sensitivity magnetometer with potassium vapour at a density of $10^{14}$ atoms/cc with buffer helium gas at several atmospheres pressure and nitrogen gas at 30 Torr to quench the potassium atoms. A schematic diagram of the experimental arrangement is shown in Figure 9. This magnetometer used a high intensity (1 W) circularly polarized pump beam along Z from a multimode laser to produce an oriented state of the atoms. The pump beam was chopped for synchronous optical pumping. A linearly polarized probe beam from a single-mode diode laser passed along the X-axis and the magnetic field was applied along the Y-axis. The probe beam was far detuned and the rotation of the plane of polarization of the probe beam was measured. The magnetic field was changed from 50 to 200 μGauss.

At these densities the spin exchange collision rate would be of the order of $10^5$/s. Yet narrow resonances were observed.

The theory of spin exchange collisions at such high densities is discussed in Walker and Happer[22]. Spin exchange collisions cause the hyperfine state of the two colliding atoms to change without a change in the expectation value of $<m_{F1}(1) + m_{F2}(2)>$. In an alkali atom the angular momenta of the two ground hyperfine states $F_1$ and $F_2$ precess in a magnetic field in opposite directions with the Larmor frequency

$$\Omega_L = g_s \mu B/[(2I + 1)\hbar]. \quad (11)$$

Here $g_s = 2$, and $I$ is the spin angular momentum of the nucleus of the atom.

When the spin relaxation rate is much larger than $\Omega_L$ (which will happen at a high density of the atoms and low magnetic field), spin exchange will cause changes in F much faster than precession. Since the state $F_1 = J + I$ has a larger statistical weight than the state $F_2 = |J - I|$, the net precession rate will not be zero, but will have a smaller value $\Omega$ given by

$$\Omega = g_s \mu B/q\hbar, \quad (12)$$

where $q = [S(S + 1) + I(I + 1)]/S(S + 1)$.

The atomic polarization will precess at this slower rate. The relaxation of the polarization will now be affected by spin-exchange processes only in the second order. Spin-exchange contribution to polarization relaxation will be small at small values of the magnetic field. The spin-destroying collisions between potassium atoms, and between potassium and helium atoms are few. Using synchronous optical pumping, one should then see a narrow magneto-optical rotation signal when the chopping frequency $\Omega_m = 2\Omega_L$. Such a signal is shown in Figure 10. The experimentally measured sensitivity was 10 fT/√Hz, with a cell 2.5 cm in diameter.

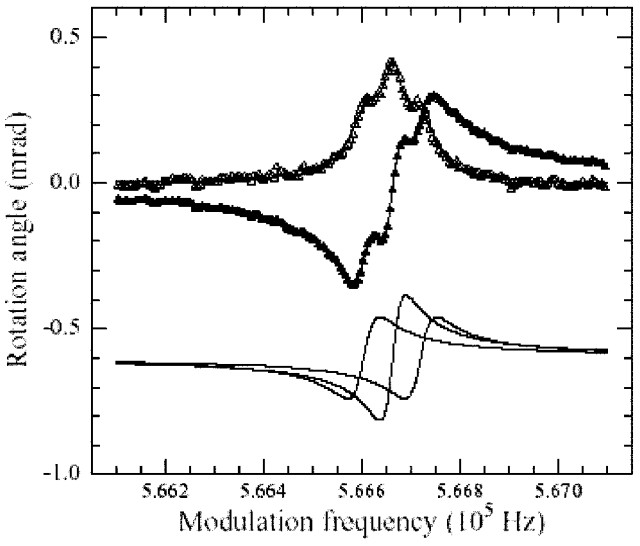


**Figure 8.** Upper traces: Optical rotation signals for $B$ = 405 mG and light power of 95 FW. Solid (hollow) triangles show the in-phase (quadrature) component. Overlaying the data is a fit to three dispersive (absorptive) Lorentzians. Lower traces: Fitted in-phase components of the three different $\Delta M_F = 2$ resonances, plotted separately. Reprinted figure from V. Acosta *et al.*, *Phys. Rev. A*, Vol. 73, 053404 (2006), with permission from D. Budker.

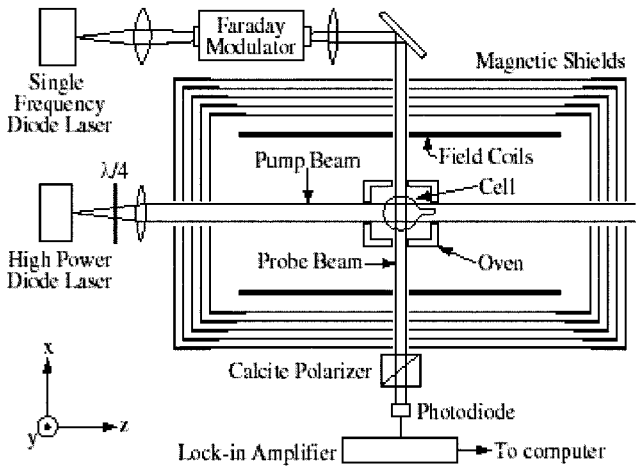


**Figure 9.** Experimental implementation of the K-magnetometer. Transverse polarization is detected using optical rotation. Reprinted figure with permission from J. C. Allred *et al. Phys. Rev. Lett.*, Vol. 89, 130801 (2002). Copyright (2002) by the American Physical Society.

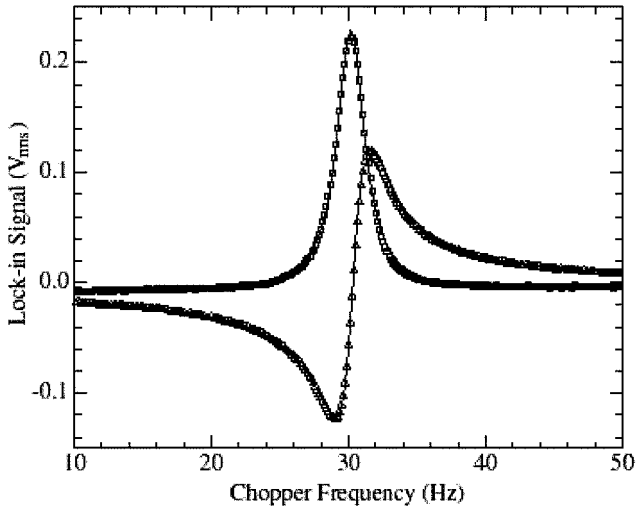


**Figure 10.** Transverse resonance of the magnetometer. Both the in-phase (squares) and out-of-phase (triangles) signals are shown. The fit is a Lorentzian with a halfwidth of 1.2 Hz. Reprinted figure with permission from J. C. Allred *et al. Phys. Rev. Lett*., Vol. 89, 130801 (2002). Copyright (2002) by the American Physical Society.


**Figure 11.** Cs-vapour microcell whose inner walls are coated with paraffin. Reprinted figure from M. V. Balabas *et al*., *J. Opt. Soc. Am. B*, Vol. 23, 1001 (2006) with permission from D. Budker.

Seltzer and Romalis[23] have described a vector magnetometer made on the above principle to measure all the components of a small magnetic field close to zero.

Subsequently, Koninis *et al.*[24] have described a seven-channel magnetometer using K. Here the expanded probe beam passes through the cell and falls on seven detector elements spaced at an interval of 3 mm. Each detector element senses an active measurement volume of 0.3 $cm^3$ of the vapour. By subtracting the signals from adjacent channels, they operated the magnetometer in the gradiometer mode. In such operation, the common mode noise in the magnetic field gets eliminated. This improved the sensitivity. These authors claim a sensitivity of 0.54 fT/√Hz in the 28 to 45 Hz range.

## Conclusion

A commercially successful magnetometer for geomagnetic and bio-magnetic applications should have the following characteristics: (i) It should have high sensitivity; (ii) it should be portable and not bulky; (iii) it should have a reasonably good spatial and temporal resolution; (iv) power consumption must be low; and (5) it should be inexpensive.

It has been amply demonstrated that a magnetometer based on NMOR can achieve sensitivity rivalling that of a Squid magnetometer. It has the advantage that no cryogenic cooling is required. It would be less expensive than a Squid magnetometer. However, most of the sensitive magnetometers using the aligned state of polarization have achieved this high sensitivity with anti-relaxation coated vapour cells having a volume of a few hundred cubic centimetres. This makes their spatial resolution limited. They would be unsuitable in the present form for biomagnetic work.

With such coatings, one should expect the polarization relaxation time to be inversely proportional to the dimension of the cell. If the cell dimension is reduced, the width of the resonance line will increase and the sensitivity will be reduced. It would be advantageous if we could make the cell size small without too much sacrifice in the sensitivity. An attempt has been made to produce Cs vapour cells with paraffin or silane coating of 3 mm diameter[25]. A photograph of such a cell is shown in Figure 11.

Both amplitude-modulated and frequency-modulated synchronous optically pumped NMOR signals were obtained with such cells. Typically, the signal had a width of about 50 μG with a laser power of 0.12 mW. The sensitivity achieved was $4 \times 10^{-8}$ G/√Hz. The sensitivity could be improved by optimizing the parameters. This is an encouraging development. However, strain-induced birefringence at the walls of the cell may pose a problem. Perhaps this can be resolved by having planar end-windows. Using micro-machining technology, miniaturization of these cells may be possible[26].

The second concern is power consumption. This may be reduced by inducing self-oscillation[27]. When the current through the laser diode was modulated in a sinusoidal fashion, it was found that the output from the balanced receiver of the frequency-modulated synchronous optical pumping magnetometer was not sinusoidal. It contained many harmonics. These harmonics had to be removed by low-pass filtering. After filtering, the phase of the signal at the first harmonic was shifted to match the phase of the AC-modulating signal to the diode. When this condition was achieved, the input AC modulator modulating the laser current could be removed and the phase-shifted low pass-filtered output from the balanced receiver could be connected to the laser diode. Self-oscillation was then achieved up to a magnetic field of 350 milli-Gauss. Low-pass filtering and phase shifting was done by both analogue and

digital means. For higher fields, the nonlinear Zeeman shifts cause a splitting of the resonance signals. Then it was difficult to get from the receiver an output signal to match in phase the AC-modulation signal. The aim is to produce anti-reflection-coated cells of 1 $mm^3$ volume. With such cells the signal will be much broader than the nonlinear Zeeman shifts. Thus, nonlinear Zeeman shifts would not pose a problem for self-oscillation. However, the sensitivity of the magnetometer would be greatly reduced.

Thus we see there are still basic problems involved in the reduction of size and of power to the NMOR-based magnetometer. Developments in the next few years will decide whether NMOR magnetometers would become commercially viable or not. However, these high sensitivity optical rotation techniques can be used in the laboratory for the study of effects important in physics, such as the search for a electrical dipole moment of an electron or atom[28] and parity nonconservation in atoms[29].

From the application point of view, one could use the NMOR technique for electromagnetic tomography (mapping of electromagnetic fields varying in space).


1. Bison, G., Weynands, R. and Weis, A., All optical magnetometer for electrocardiography. *Appl. Phys*., 2003, **B76**, 375.
2. Budker, D., Gawlik, W., Kimball, D. F., Rochester, S. M., Yashchuk, V. V. and Weis, A., Resonant nonlinear magneto-optical effects in atoms. *Rev. Mod. Phys*., 2002, **74**, 1153.
3. Alexandrov, E. B., Auzinsch, M., Budker, D., Kimball, D. F., Rochester, S. M. and Yashchuk, V. V., Dynamic effects in nonlinear magneto-optics of atoms and molecules: Review. *J. Opt. Soc. Am. B*, 2005, **22**, 7.
4. Rochester, S. M. and Budker, D., Atomic polarization visualized. *Am. J. Phys*., 2002, **60**, 450.
5. Macaluso, D. and Corbino, O. M., *C.R. Hebd Seances Acad. Sci*., 1898, **127**, 548.
6. Kanorsky, S. I., Weis, A., Wurster, J. and Hänsch, T. W., Quantitative investigation of the resonant nonlinear Faraday effect under conditions of optical hyperfine pumping. *Phys. Rev. A*, 1993, **47**, 1220.
7. Schuh, B., Kanorsky, S. I., Weis, A. and Hänsch, T., Observation of Ramsey fringes in nonlinear Faraday rotation. *Opt. Commun*., 1993, **100**, 451.
8. Labeyrie, G., Miniatura, C. and Kaiser, R., Large Faraday rotation of resonant light in a cold atomic cloud. *Phys. Rev. A*, 2001, **64**, 033402.
9. Franke-Arnold, S., Arndt, M. and Zeilinger, A., Magneto-optical effects with cold lithium atoms. *J. Phys. B*, 2001, **34**, 2527.
10. Robinson, H. G., Ensberg, E. S. and Dehmelt, H. G., *Bull. Am. Phys. Soc*., 1958, **3**, 9.
11. Alexandrov, E. B. and Bonch-Bruevich, V. A., Experimental realization of coherent dark state magnetometers. *Opt. Eng*., 1992, **31**, 711.
12. Budker, D., Hollberg, L., Kimball, D. F., Kitching, J., Pustelny, S. and Yashchuk, V. V., Microwave transitions and nonlinear magneto-optical rotation in anti-relaxation-coated cells. *Phys. Rev. A*, 2005, **71**, 012903.
13. Kanorskii, S. I., Weis, A. and Skalla, J., A wall collision induced Ramsey Resonance. *Appl. Phys. B*, 1995, **60**, S165.
14. Budker, D., Yashchuk, V. and Zolotorev, M., Nonlinear magneto-optic effects with ultranarrow widths. *Phys. Rev. Lett.*, 1998, **81**, 5788.
15. Budker, D., Kimball, D. F., Yashchuk, V. V. and Zolotorev, M., Nonlinear magneto-optical rotation with frequency-modulated light. *Phys. Rev. A*, 2003, **65**, 055403.
16. Sautenkov, V. A. *et al*., Enhancement of magneto-optic effects via large atomic coherence in optically dense media. *Phys. Rev. A*, 2000, **62**, 023810.
17. Bell, W. E. and Bloom, A. L., Optically driven spin precession. *Phys. Rev. Lett.*, 1961, **6**, 280.
18. Budker, D., Kimball, D. F., Rochester, S. M., Yashchuk, V. V. and Zolotorev, M., Sensitive magnetometry based on nonlinear magneto-optical rotation. *Phys. Rev. A*, 2000, **62**, 043403.
19. Yashchuk, V., Budker, D. and Zolotorev, M., Nonlinear magneto-optical effects with ultra-narrow widths. Preprint LBNL 042228, 1998.
20. Acosta, V. *et al*., Nonlinear magneto-optical rotation with frequency-modulated light in the geophysical field range. *Phys. Rev. A*, 2006, **73**, 053404.
21. Allred, J. C., Lyman, R. N., Kornack, T. W. and Romalis, M. V., High-sensitivity atomic magnetometer unaffected by spin-exchange relaxation. *Phys. Rev. Lett*., 2002, **89**, 130801.
22. Walker, T. G. and Happer, W., Spin-exchange optical pumping of noble-gas nuclei. *Rev. Mod. Phys*., 1997, **69**, 629.
23. Selzer, S. J. and Romalis, M. V., Unshielded three axis vector operation of a spin-exchange-relaxation-free atomic magnetometer. *Appl. Phys. Lett.*, 2004, **85**, 4804.
24. Koninis, L. E., Komack, T. W., Alfred, J. C. and Romalls, M. V., A sub-femto-tesla multichannel atomic magnetometer. *Nature*, 2003, **422**, 596.
25. Balabas, M. V., Budker, D., Kitching, J., Schwindt, P. D. D. and Stalnaker, J. E., Magnetometry with millimeter-scale antirelaxation-coated alkali-metal vapor cells. *J. Opt. Soc. Am. B*, 2006, **23**, 1001.
26. Kitching, J., Knappe, S. and Hollberg, L., Miniature vapor-cell atomic-frequency references. *Appl. Phys. Lett.*, 2002, **81**, 553.
27. Schwindt, P. D. D., Holberg, L. and Kitching, J., Self-oscillating rubidium magnetometer using nonlinear magneto-optical rotation. *Rev. Sci. Instrum*., 2005, **76**, 126–103.
28. Kimball, D. F., Budker, D., English, D. F., Lee, C. H., Nguyen, A. T., Rochester, S. M., Sushkov, A., Yashchuk, V. M. and Zolotorev, M., Progress towards fundamental symmetry tests using non-linear optical rotation. In *Festschrift for Eugene D. Cummins* (eds Budker, D., Friedman, D. and Bucksbaum, Ph.), AIP, 2001, pp. 84–107.
29. Bouchiat, M. A. and Bouchiat, C., Parity violation in atoms. *Rep. Prog. Phys*., 1997, **60**, 1351.


ACKNOWLEDEGMENT. I thank the referee for his helpful comments.

Received 18 May 2006; revised accepted 3 October 2006